short-lived transient decreases in intensity relative to the long-lived emission component upon increasing [Fe(II)]:[Ru(II)] above 4:1. Because experiments are performed by adding Fe(II) to solutions having a fixed concentration of complexes **1a–4a**, the dissociation of the product complex **1b–4b** to form $\{[(bpy)_2Ru(L\text{-}L)]_2Fe(S)_2\}$, where S is solvent, becomes important at high concentrations of iron(II). The resulting high-spin iron(II) complex should be a weaker quencher of excited ruthenium bipyridyl centers than the low-spin iron complexes **1b–4b**. For $[Fe(bpy)_3]^{2+}$ the analogous reaction, shown in eq 4, has an equilibrium constant of 10^{-8}.[13]

$$2[Fe(bpy)_3]^{2+} + [Fe(OH_2)_6]^{2+} \rightleftarrows 3[Fe(bpy)_2(OH_2)_2]^{2+} \quad (4)$$

However, for **1b–4b** the constant for this process should be much higher since there are significant steric and coulombic repulsion factors for the "ligands" **1a–4a**. The decrease in K_{eq} for formation of **1b–4b** with decreasing bridge length, R, supports a process similar to eq 4 as the mechanism for the decrease in quenching at high [Fe(II)]. Further, a decrease in the absorbance due to **1b–4b** at 525 nm is observed at high [Fe(II)]. As a result, the degree of emission quenching at high [Fe(II)] decreases and the limiting $\phi_{complex}/\phi^\circ_{free}$ (Figure 3) value does not reflect complete complexation of **1a–4a** to form **1b–4b**. Since $\tau_{complex}/\tau^\circ_{free}$, represents the limiting value for lifetimes, it is much smaller than $\phi_{complex}/\phi^\circ_{free}$ for each complex.

Conclusion

This work demonstrates that uncomplexed bipyridines covalently attached in tris(bipyridyl)ruthenium(II) derivatives can be effectively used as ligands for complexation to other metals to prepare polynuclear clusters having high charge. In situ preparation of the tris Fe(II) complexes **1b–4b** only partially quenches the ruthenium bipyridyl emission via energy transfer. Communication between the ruthenium bipyridyl donor and the iron bipyridyl acceptor depends on the length of the covalent linkage between the two centers.

Acknowledgment. Support by the National Science Foundation (Grant CHE-8214299) is gratefully acknowledged (C.M.E.). Acknowledgment is also made to the donors of the Petroleum Research Fund (R.H.S. and R.A.A.), administered by the American Chemical Society, for partial support of this work.

Contribution from the Guelph Waterloo Centre for Graduate Work in Chemistry, Guelph Campus,
Department of Chemistry and Biochemistry, University of Guelph, Guelph, Ontario N1G 2W1, Canada,
and Department of Chemistry, University of Arkansas, Fayetteville, Arkansas 72701

Redox Chemistry of 1,2,4,6-Thiatriazinyls: Preparation and Crystal Structures of 3,5-Diphenyl-1,2,4,6-thiatriazinium Hexafluorophosphate, $[Ph_2C_2N_3S]^+[PF_6]^-$, and 3,5-Diphenyl-4-hydro-1,2,4,6-thiatriazine, $[Ph_2C_2N_3SH]$

René T. Boeré,[1a] A. Wallace Cordes,[1b] Patrick J. Hayes,[1a] Richard T. Oakley,*[1a] Robert W. Reed,[1a]
and William T. Pennington[1b]

Received December 5, 1985

The oxidation of 3,5-diphenyl-1,2,4,6-thiatriazinyl dimer with the nitrosonium salts $[NO]^+X^-$ ($X^- = BF_4^-, PF_6^-$) yields the corresponding salts of the $[Ph_2C_2N_3S]^+$ cation. Reduction of the same compound by sodium in liquid ammonia affords, following acidification, the reduced system 3,5-diphenyl-4-hydro-1,2,4,6-thiatriazine, $Ph_2C_2N_3SH$. The structures of $[Ph_2C_2N_3S]^+[PF_6]^-$ and $Ph_2C_2N_3SH{\cdot}0.5CH_2Cl_2$ have been determined by X-ray diffraction. The structural parameters of the triad of oxidation states of the C_2N_3S ring system, i.e. cation, radical dimer, and anion, are discussed in relation to the results of MNDO molecular orbital calculations on model compounds related to the three species. Crystals of $[Ph_2C_2N_3S]^+[PF_6]^-$ are monoclinic, space group $C2/c$, with $a = 18.170$ (4) Å, $b = 12.080$ (2) Å, $c = 7.748$ (3) Å, $\beta = 108.56$ (4)°, $V = 1612$ (2) Å^3, and $Z = 4$ at 22 °C and $R = 0.064$ for 1114 reflections with $I > 3\sigma(I)$. Crystals of $Ph_2C_2N_3SH{\cdot}0.5CH_2Cl_2$ are orthorhombic, space group $Pbcn$, with $a = 19.427$ (3) Å, $b = 9.900$ (2) Å, $c = 14.840$ (4) Å, $\beta = 90°$, $V = 2854$ (2) Å^3, and $Z = 8$ at 22 °C and $R = 0.047$ for 1152 reflections with $I > 3\sigma(I)$.

Introduction

The redox chemistry of binary sulfur nitride molecules and ions has been studied extensively. The electrochemical and chemical reduction of S_4N_4[2,3] leads via the radical anion $S_4N_4^-$[3] to the cyclic $S_3N_3^-$[4] ion, while its oxidation in strongly acidic media affords, inter alia, the dication $S_4N_4^{2+}$[5] and the radical $S_3N_2^+$[6] cation. A radical cation $S_4N_4^+$ has recently been postulated, but no spectroscopic evidence was provided.[7] Neutral radical systems are less common. Although the existence of the $S_3N_3^\bullet$ radical in the gas phase has been clearly demonstrated,[8] attempts to observe it in solution have been unsuccessful; both oxidation of $S_3N_3^-$ and reduction of $S_3N_3Cl_3$ yield S_4N_4.[2b,9] Because of this propensity of SN molecules and ions to undergo drastic structural rearrangements following electron transfer, their potential applications in the design of devices and electrocatalysts is limited.

One approach to remedying the structural instability of binary sulfur–nitrogen radicals is to modify them through incorporation of organic units. Several neutral organothiazyl radicals have now been characterized,[10–15] including the remarkably stable 3,5-di-

---

(1) (a) University of Guelph. (b) University of Arkansas.

(2) (a) Hojo, M. *Bull. Chem. Soc. Jpn.* **1980**, *53*, 2856. (b) Chivers, T.; Hojo, M. *Inorg. Chem.* **1984**, *23*, 1526. (c) Tweh, J. W.; Turner, A. G. *Inorg. Chim. Acta* **1981**, *48*, 173.

(3) (a) Brown, O. R. *J. Electroanal. Chem. Interfacial Electrochem.* **1972**, *34*, 419. (b) Williford, J. D.; Van Reet, R. E.; Eastman, M. P.; Prater, K. B. *J. Electrochem. Soc.* **1973**, *120*, 1498.

(4) Bojes, J.; Chivers, T.; Laidlaw, W. G.; Trsic, M. *J. Am. Chem. Soc.* **1979**, *101*, 4517.

(5) Gillespie, R. J.; Kent, J. P.; Sawyer, J. F.; Slim, D. R.; Tyrer, J. D. *Inorg. Chem.* **1981**, *20*, 3799.

(6) (a) Gillespie, R. J.; Kent, J. P.; Sawyer, J. F. *Inorg. Chem.* **1981**, *20*, 4053. (b) Roesky, H. W.; Hamza, A. *Angew. Chem., Int. Ed. Engl.* **1976**, *15*, 226. (c) Krebs, B.; Henkel, G.; Pohl, S.; Roesky, H. W. *Chem. Ber.* **1980**, *113*, 226.

(7) Muller, U.; Conradi, E.; Emart, U.; Dehnicke, K. *Angew. Chem., Int. Ed. Engl.* **1984**, *23*, 237.

(8) (a) Lau, W. M.; Westwood, N. P. C.; Palmer, M. C. *J. Chem. Soc., Chem. Commun.* **1985**, 752. (b) Lau, W. M.; Westwood, N. P. C.; Palmer, M. C. *J. Am. Chem. Soc.*, in press.

(9) Oakley, R. T., unpublished results.

(10) Wolmershäuser, G.; Schnauber, M.; Wilhelm, T. *J. Chem. Soc., Chem. Commun.* **1984**, 573.

(11) (a) Fairhust, S. A.; Pilkington, R. S.; Sutcliffe, L. H. *J. Chem. Soc., Faraday Trans. 1* **1983**, *79*, 439, 925. (b) MacLean, G. K.; Passmore, J.; Schriver, M. J.; White, P. S.; Bethell, D.; Pilkington, R. S.; Sutcliffe, L. H. *J. Chem. Soc., Chem. Commun.* **1983**, 807.

(12) Kaplan, M. L; Haddon, R. C.; Hirani, A. M.; Schilling, F. C.; Marshall, J. H. *J. Org. Chem.* **1981**, *46*, 675.

(13) Banister, A. J.; Smith, N. R. M.; Hey, R. G. *J. Chem. Soc., Perkin Trans 1* **1983**, 1181.

Scheme I

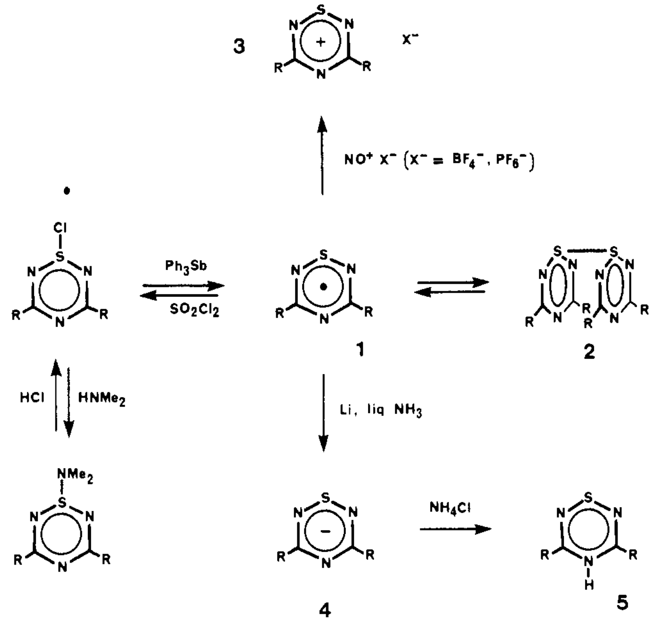

phenyl-1,2,3,6-thiatriazinyl system **1**, which, in the solid state, exists as the cofacial dimer **2**.[15] In order to probe the structural stability of this radical with respect to redox changes, we have pursued the characterization of its cationic and anionic redox partners **3** and **4**. In the present paper we describe the preparation and molecular structures of 3,5-diphenyl-1,2,4,6-thiatriazinium hexafluorophosphate, $[Ph_2C_2N_3S]^+[PF_6]^-$, and 3,5-diphenyl-4-hydro-1,2,4,6-thiatriazine, $Ph_2C_2N_3SH$ (**5**), the protonated form of **4**. Their structures are discussed in the light of MNDO molecular orbital calculations on model structures.

Experimental Section

Starting Materials and General Procedures. The 3,5-diphenyl-1,2,4,6-thiatriazinyl dimer **2** was prepared as recently described by the reduction of 1-chloro-3,5-diphenyl-1,2,4,6-thiatriazine with triphenylantimony.[15] Nitrosyl tetrafluoroborate, $NOBF_4$, and hexafluorophosphate, $NOPF_6$ (Aldrich), were sublimed in vacuo, and sulfuryl chloride (Aldrich) was distilled before use. Sodium metal (Alfa), ammonia and hydrogen chloride gas (Matheson), and (dimethylamino)trimethylsilane (Petrarch) were used as received. Acetonitrile (Fisher, HPLC grade) was purified by distillation from phosphorus pentoxide and calcium hydride. Diethyl ether (Fisher absolute) was dried by distillation from lithium aluminum hydride. Infrared spectra were recorded on Nujol mulls (with CsI cells) with a Perkin-Elmer 1330 grating spetrophotometer, and UV–vis spectra were obtained with a Hewlett-Packard 845A diode array spectrophotometer. Mass spectra were recorded on a VG 7070 mass spectrometer by electron impact at 70 eV, samples being admitted through conventional inlet systems. ^1H NMR spectra were recorded on a Bruker WH-400 spectrometer. Melting points (uncorrected) were measured on a Gallenkamp melting point apparatus. Chemical analyses were performed by MHW Laboratories, Phoenix, AZ. All synthetic procedures were carried out under an atmosphere of nitrogen gas.

Preparation of $[Ph_2C_2N_3S]^+[BF_4]^-$ (3a). A slurry of **2** (0.365 g, 0.723 mmol) and nitrosyl tetrafluoroborate (0.190 g, 1.63 mmol) in acetonitrile was stirred and heated at reflux for 2 h to yield a clear red solution from which orange red crystalline needles precipitated on cooling. The extremely moisture-sensitive crystals of $[Ph_2C_2N_3S]^+[BF_4]^-$ (**3a**; 0.235 g, 0.693 mmol, 48%) dec pt >230 °C, were collected by filtration under nitrogen. Anal. Calcd for $C_{14}H_{10}N_3SBF_4$: C, 49.59; H, 2.97; N, 12.39. Found: C, 49.39; H, 3.02; N, 12.11. Mass spectrum (*m/e*): 252 ($Ph_2C_2N_3S^+$, 48%), 149 ($PhCN_2S^+$, 25%), 103 ($PhCN^+$, 45%), 77 (Ph^+, 10%), 49 (BF_2^+, 56%), 46 (SN^+, 100%). Infrared spectrum (1600–250-cm^{-1} region): 1595 (vs), 1495 (vw), 1300 (w), 1265 (w), 1180 (m), 1110 (vs, b, unresolved), 1000 (w), 970 (m), 735 (vs), 675 (vs), 610 (s), 550 (m), 525 (w), 500 (w) cm^{-1}.

Preparation of $[Ph_2C_2N_3S]^+[PF_6]^-$ (3b). This salt was prepared in a manner entirely analogous to that described above for **3a**. Infrared spectrum (1600–250-cm^{-1} region): 1586 (m), 1480 (vw), 1435 (vs), 1387 (s), 1288 (w), 1258 (w), 1173 (m), 1098 (w), 990 (w), 959 (m), 824 (s, br), 797 (w), 729 (s), 666 (m), 600 (m), 554 (m).

Preparation of $Ph_2C_2N_3SH$ (5). Sodium (0.192 g, 8.35 mmol) was added, in small pieces, to a slurry of $(Ph_2C_2N_3S)_2$ (**1**; 2.00 g, 3.97 mmol) in 150 mL of liquid ammonia. After 45 min anhydrous ammonium chloride (0.423 g, 7.92 mmol) was added and the solvent allowed to evaporate under a stream of nitrogen. The residual solid was extracted into 100 mL of CH_2Cl_2 and the red solution flash chromatographed through a short silica plug, which was flushed with sufficient solvent to ensure the removal of all colored material. Evaporation of the solvent from the eluate gave a red crystalline solid, which could be recrystallized from a CH_2Cl_2/hexane mixture as red needles of the solvate $Ph_2C_2N_3SH{\cdot}0.5CH_2Cl_2$ (0.91 g, 3.1 mmol, 39%), mp 134–136 °C. The unsolvated material $Ph_2C_2N_3SH$ (**5**) was obtained for analytical purposes by heating the solvate at 60 °C (0.01 torr) for 4 h. Anal. Calcd for $C_{14}H_{11}N_3S$: C, 66.67; H, 3.97; N, 16.67. Found: C, 66.41; H, 4.09; N, 16.45. UV–vis spectrum (CH_2Cl_2, λ_{max} (log ϵ)): 474 (3.0) nm. Infrared spectrum: 3210 (br) cm^{-1} (ν(NH)); 1638 (vs), 1590 (m) 1568 (s), 1450 (vs), 1415 (s), 1255 (s), 1158 (w), 1100 (br, w), 1075 (w), 1050 (w), 1022 (w), 975 (w), 770 (s), 720 (m), 688 (s), 679 (s), 660 (s), 610 (m), 465 (w), 270 (w), 240 (w) cm^{-1} (1600–250-cm^{-1} region). Mass spectrum (*m/e*): 253 ($Ph_2C_2N_3SH^+$, 19%), 252 ($Ph_2C_2N_3S^+$, 38%), 149 ($PhCN_2S^+$, 24%), 104 ($PhCNH^+$, 43%), 103 ($PhCN^+$, 63%), 77 (Ph^+, 20%), 46 (SN^+, 100%).

Oxidation of $(Ph_2C_2N_3S)_2$ (2) with Sulfuryl Chloride. An excess of sulfuryl chloride (0.88 g, 0.66 mmol) in 2 mL of acetonitrile was injected into a slurry of $(Ph_2C_2N_3S)_2$ (**2**; 0.250 g, 0.495 mmol) in 10 mL of CH_3CN. An immediate color change occurred, resulting in the formation of a yellow solid and a yellow supernatant solution. The mixture was heated to dissolve the solid, and upon cooling, yellow needles of $Ph_2C_2N_3SCl$ (0.222 g, 0.772 mmol, 78%) were obtained. These were isolated by filtration under nitrogen and characterized by their infrared spectrum and melting point.

Oxidation of $Ph_2C_2N_3SH$ with Sulfuryl Chloride. Sulfuryl chloride (75 μL, 0.13 g, 0.93 mmol) was injected into a solution of $Ph_2C_2N_3SH$ (0.21 g, 0.83 mmol) in 5 mL of acetonitrile. The red color of the solution was instantly discharged, leaving a pale yellow solution from which a pale yellow crystalline solid appeared. The solid was filtered off and identified as $Ph_2C_2N_3SCl$ (0.13 g, 0.45 mmol, 55%) by its infrared spectrum and melting point.

Preparation of $Ph_2C_2N_3SNMe_2$. A solution of Me_2NSiMe_3 (0.81 g, 6.91 mmol) in 25 mL of CH_2Cl_2 was added dropwise with stirring to a solution of $Ph_2C_2N_3SCl$ (1.80 g, 6.26 mmol) in 75 mL of CH_2Cl_2. After 16 h the solvent was removed in vacuo to leave a pale yellow solid, which was recrystallized from hot acetonitrile as bright yellow trapezoidal plates (1.85 g, 6.24 mmol), mp 97–99 °C. Anal. Calcd for $C_{16}H_{16}N_4S$: C, 64.84; H, 5.44; N, 18.90. Found: C, 64.78; H, 5.50, N, 19.05. Mass spectrum (*m/e*): 252 ($Ph_2C_2N_3S^+$, 100%), 149 ($PhCN_2S^+$, 39%), 103 ($PhCN^+$, 25%), 46 (SN^+, 90%). ^1H NMR spectrum ($CDCl_3$): δ 2.69 (s, 6 H, NMe_2), 7.0–8.0 (m, 10 H, Ph). Infrared spectrum (1600–250-cm^{-1} region): 1490 (s, br), 1450 (s), 1375 (vs, br) 1340 (s), 1320 (m), 1285 (m), 1190 (m), 1145 (w), 1075 (w), 1020 (w), 925 (s), 815 (w), 790 (m), 760 (w), 730 (vs), 690 (m), 670 (w), 660 (w), 610 (w), 435 (w) cm^{-1}.

Reaction of $Ph_2C_2N_3SNMe_2$ with Hydrogen Chloride. Anhydrous hydrogen chloride was passed through a solution of $Ph_2C_2N_3SNMe_2$ (0.70 g, 2.36 mmol) in 50 mL of ether, resulting in the immediate precipitation of a white solid. The mixture was filtered and the filtrate reduced to dryness in vacuo to leave a pale yellow solid. Extraction of this solid with 20 mL of hot carbon tetrachloride, filtration of the extract, and removal of the solvent from the filtrate yielded crystalline $Ph_2C_2N_3SCl$ (0.30 g, 1.04 mmol, 46%), identified by its infrared spectrum and melting point.

X-ray Measurements. A crystal of **3b** was mounted under nitrogen in a glass capillary, while a sample of **5** was attached to a glass fiber with epoxy (Table IA). X-ray data were collected with an Enraf-Nonius CAD-4 diffractometer employing graphite-monochromated Mo Kα (λ = 0.71073 Å) radiation. Data collection parameters are listed in Table IB.

The structures were solved by direct methods (MULTAN11/82)[16] and

---

(14) Höfs, H.-U.; Bats, J. W.; Gleiter, R.; Hartmann, G.; Mews, R.; Eckert-Maksić, M.; Oberhammer, H.; Sheldrick, G. M. *Chem. Ber.* **1985**, *118*, 3781.

(15) (a) Cordes, A. W.; Hayes, P. J.; Josephy, P. D.; Koenig, H.; Oakley, R. T.; Pennington, W. T. *J. Chem. Soc., Chem. Commun.* **1984**, 1021. (b) Hayes, P. J.; Oakley, R. T.; Cordes, A. W.; Pennington, W. T. *J. Am. Chem. Soc.* **1985**, *107*, 1346.

(16) Main, P. "MULTAN/82, a System of Computer Programs for the Automatic Solution of Crystal Structures from X-ray Diffraction Data"; University of York, York, England, 1982.

Table I. Data for the Structure Determinations of $Ph_2C_2SN_3H{\cdot}0.5CH_2Cl_2$ (**5**) and $[Ph_2C_2SN_3]^+[PF_6]^-$ (**3b**)

	5	**3b**
	A. Crystal Data	
formula	$C_{14.5}H_{12}SN_3Cl$	$C_{14}H_{10}PF_6SN_3$
fw	295.8	397.3
cryst syst	orthorhombic	monoclinic
space group	*Pbcn*	*C*2/*c*
no. of reflecns in cell detn	25	25
a, Å	19.427 (3)	18.170 (4)
b, Å	9.900 (2)	12.080 (2)
c, Å	14.840 (4)	7.748 (3)
β, deg	90	108.56 (4)
V, Å^3	2854 (2)	1612 (2)
D_{calcd}, g cm^{-3}	1.38	1.64
μ(Mo Kα), cm^{-1}	4.0	3.5
Z	8	4
size, mm	0.20 × 0.36 × 0.46	0.24 × 0.27 × 0.98
total decay, %	14.8	0.5
abs cor	0.94–1.00	0.96–1.00
	B. Data Collection and Refinement	
total unique reflecns	2967	1413
obsd data ($I > 3\sigma(I)$)	1152	1114
params refined	181	115
R	0.047	0.064
R_w	0.061	0.089
GOF	2.3	2.51
reflecn/param ratio	6.4/1	9.7/1
max shift/error	0.01	0.02
final diff map max, e Å^{-3}	±0.2	+0.5, −0.4
p factor of counting statistics for wts	0.04	0.05

Table II. Atom Coordinates for **3b**[a]

atom	*x*	*y*	*z*	*B*, Å^2
S	0.500	0.8525 (1)	0.250	4.86 (4)
P	0.500	0.1883 (1)	0.250	3.95 (4)
F(1)	0.5176 (2)	0.2790 (3)	0.1252 (4)	9.5 (1)
F(2)	0.5200 (3)	0.0977 (3)	0.1265 (5)	11.6 (1)
F(3)	0.5843 (2)	0.1906 (6)	0.3777 (6)	13.8 (2)
N(1)	0.4265 (2)	0.7817 (3)	0.2140 (5)	4.14 (8)
N(2)	0.500	0.6157 (4)	0.250	3.6 (1)
C(1)	0.4330 (2)	0.6688 (4)	0.2229 (5)	3.46 (9)
C(2)	0.3629 (2)	0.6050 (4)	0.1995 (6)	4.0 (1)
C(3)	0.2938 (3)	0.6587 (4)	0.1891 (7)	5.2 (1)
C(4)	0.2272 (3)	0.5975 (5)	0.1670 (8)	6.6 (1)
C(5)	0.2290 (3)	0.4852 (5)	0.1556 (9)	6.8 (2)
C(6)	0.2971 (3)	0.4304 (5)	0.1655 (9)	6.5 (2)
C(7)	0.3645 (2)	0.4906 (1)	0.1886 (7)	4.9 (1)

[a] Anisotropically refined atoms are given in the form of the isotropic equivalent thermal parameter defined as $^4/_3[a^2B_{11} + b^2B_{22} + c^2B_{33} + ab(\cos\gamma)B_{12} + ac(\cos\beta)B_{13} + bc(\cos\alpha)B_{23}]$.

refined (Table IB) by full-matrix least-squares analyses based on $(|F_o| - |F_c|)^2$. The nitrogen-bonded hydrogen atom position and its isotropic temperature factor were refined in **3b**; phenyl ring hydrogen atoms were constrained to idealized (C–H = 0.95 Å) positions in both structures, with isotropic temperature factors 1.2 times those of the carbon atoms to which they are bonded. Weighting schemes gave no systematic variation in $F/\sigma(F)$ as a function of F or sin θ. No secondary extinction corrections were made. Neutral-atom scattering factors[17] were corrected for real and imaginary anomalous dispersion.[18] The computer programs used were those provided with the Enraf-Nonius structure determination package. Atom coordinates for **3b** and **5** are given in Tables II and III, and bond distance and angle information is provided in Table IV. Tables containing the anisotropic thermal parameters of **3b** and **5** have been deposited as supplementary material.

Theoretical Method and Models. The MNDO (modified neglect of diatomic overlap) method[19] has been used extensively for studying the structural properties of binary thiazyl compounds and related derivatives. Comparative calculations on the electronic structures of **1**, **3**, **4**, and **5** were carried out by using the MOPAC program[19b] and model compounds in which the exocyclic phenyl groups were replaced by hydrogens. Full geometry optimization, within the confines of C_{2v} symmetry, was invoked for each molecule. In the case of the radical $H_2C_2N_3S{\cdot}$, the restricted Hartree–Fock calculation was based on the half-electron model. Bond orders and charge densities refer to the elements of the Coulson charge density matrix.

Table III. Atom Coordinates for **5**

atom	*x*	*y*	*z*	*B*, Å^2
S	0.12425 (8)	0.1633 (2)	0.0477 (1)	4.86 (4)
N(1)	0.2087 (2)	0.1337 (5)	0.0274 (3)	3.7 (1)
N(2)	0.2254 (2)	0.3609 (5)	0.0641 (3)	3.7 (1)
N(3)	0.1227 (3)	0.2861 (5)	0.1275 (4)	4.5 (1)
C(1)	0.2492 (3)	0.2359 (6)	0.0344 (4)	3.2 (1)
C(2)	0.3221 (3)	0.2228 (6)	0.0144 (4)	3.3 (1)
C(3)	0.3717 (3)	0.3018 (6)	0.0558 (5)	4.6 (2)
C(4)	0.4401 (3)	0.2802 (7)	0.0409 (5)	6.0 (2)
C(5)	0.4612 (4)	0.1785 (7)	−0.0157 (6)	7.0 (2)
C(6)	0.4129 (4)	0.1015 (7)	−0.0591 (6)	6.5 (2)
C(7)	0.3439 (3)	0.1227 (6)	−0.0457 (5)	4.6 (2)
C(8)	0.1716 (3)	0.3715 (6)	0.1243 (4)	3.7 (1)
C(9)	0.1735 (3)	0.4862 (6)	0.1872 (4)	4.1 (1)
C(10)	0.1115 (4)	0.5451 (1)	0.2135 (5)	5.8 (2)
C(11)	0.1135 (4)	0.6554 (7)	0.2725 (5)	7.4 (2)
C(12)	0.1742 (5)	0.7037 (8)	0.3051 (5)	7.1 (2)
C(13)	0.2348 (4)	0.6456 (7)	0.2807 (4)	6.6 (2)
C(14)	0.2353 (4)	0.5356 (6)	0.2224 (4)	5.2 (2)
C(15)	0.000	0.118 (1)	0.250	13.0 (4)
Cl	0.0618 (2)	0.0242 (4)	0.3033 (3)	16.3 (1)

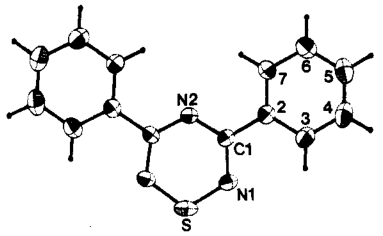

Figure 1. ORTEP drawing (30% probability ellipsoids) of the cation in **3b**, showing the atom-numbering scheme.

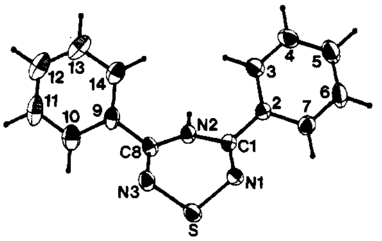

Figure 2. ORTEP drawing (30% probability ellipsoids) of **5**, showing the atom-numbering scheme.

Results and Discussion

Preparation of $[Ph_2C_2N_3S]^+X^-$ ($X^- = BF_4^-$, PF_6^-) and $Ph_2C_2N_3SH$. The structural stability of the 1,2,4,6-thiatriazinyl radical **1** is in marked contrast to the behavior of the radicals generated from binary SN radical systems. In the hope that the cyclic C_2N_3S skeleton of **1** would remain stable over a range of oxidation states, we have studied its reactions with strong oxidants and reductants. In particular we were concerned about the accessibility of the 8π-electron anion **4**. We have found that **1** can be reduced by sodium or lithium in liquid ammonia. Although we have been unable to isolate the anion **4** itself, we have successfully characterized the imide **5** by acidification of the reduced solution in ammonia with ammonium chloride. Both the imide **5** and the radical **1** can be converted into the oxidized 1-chloro-3,5-diphenyl-1,2,4,6-thiatriazine by treatment with sulfuryl chloride. Reaction of **2** with nitrosyl tetrafluoroborate or hexafluorophosphate generates the corresponding ionic salt $[Ph_2C_2N_3S]^+X^-$ ($X^- = BF_4^-$ (**3a**) or PF_6^- (**3b**)). The substitution

---

(17) Cromer, D. T.; Waber, J. T. *International Tables for X-ray Crystallography*; Kynoch: Birmingham, England, 1974; Vol. IV, Table 2.2B.

(18) Cromer, D. T. *International Tables for X-ray Crystallography*; Kynoch: Birmingham, England, 1974; Vol. IV, Table 2.3.1.

(19) (a) Dewar, M. J. S.; Thiel, W. *J. Am. Chem. Soc.* **1977**, *99*, 4899. (b) *QCPE* **1984**, *No. 455* (MOPAC).

Table IV. Selected Bond Lengths (in Å) and Angles (in deg) for **3b** and **5**

atom 1	atom 2	**5**	**3b**
S	N(1)	1.694 (3)	1.535 (3)
S	N(3)	1.598 (4)	
N(1)	C(1)	1.285 (5)	1.369 (4)
N(2)	C(1)	1.393 (5)	1.332 (3)
N(2)	C(8)	1.380 (5)	
N(2)	H(N2)	0.83 (4)	
N(3)	C(8)	1.273 (5)	
C(1)	C(2)	1.453 (6)	1.450 (4)
C(8)	C(9)	1.471 (6)	
C(15)	Cl	1.712 (5)	
P	F(1)		1.560 (2)
P	F(2)		1.571 (2)
P	F(3)		1.537 (2)
C	C (Ph)	1.359–1.400 1.380 (av)	1.360–1.392 1.381 (av)

atom 1	atom 2	atom 3	**5**	**3b**
N(1)	S	N(3)	105.4 (2)	112.3 (2)
S	N(1)	C(1)	116.2 (3)	119.3 (2)
C(1)	N(2)	C(8)	121.5 (4)	122.4 (4)
C(1)	N(2)	H(N2)	113 (3)	
C(8)	N(2)	H(N2)	123 (3)	
S	N(3)	C(8)	115.9 (3)	
N(1)	C(1)	N(2)	121.5 (4)	123.2 (3)
N(1)	C(1)	C(2)	120.6 (4)	117.7 (3)
N(2)	C(1)	C(2)	117.8 (4)	119.1 (3)
C(1)	C(2)	C(3)	122.5 (4)	120.0 (3)
C(1)	C(2)	C(7)	119.2 (4)	120.2 (3)
N(2)	C(8)	N(3)	122.7 (4)	
N(2)	C(8)	C(9)	116.8 (4)	
N(3)	C(8)	C(9)	120.5 (4)	
C(8)	C(9)	C(10)	118.6 (5)	
C(8)	C(9)	C(14)	122.0 (4)	
C	C	C (Pheny)	118.2–121.0	119.6–120.8
F	P	F		178.0–178.53, 87.0–91.7

Table V. Mean Endocyclic Distances (in Å) in Selected 1,2,4,6-Thiatriazines

compd	$S-N_{2,6}$	$N_{2,6}-C$	$C-N_4$	ref
$Cl_2C_2N_3SN(i\text{-}Pr)_2$	1.655	1.300	1.329	20
$Ph_2C_2N_3SCl$	1.59	1.34	1.34	15a
3b	1.535	1.369	1.332	this work
2	1.62	1.33	1.34	15b
5	1.65	1.28	1.39	this work

chemistry of the *S*-chloro derivative has been explored by simple amination, with Me_3SiNMe_2, to the *S*-dimethylamino derivative. This "protecting" group can be easily removed from sulfur by treatment with anhydrous hydrogen chloride. The transformations described above are summarized in Scheme I.

Molecular Structures of $[Ph_2C_2N_3S]^+[PF_6]^-$ and $Ph_2C_2N_3SH\cdot 0.5CH_2Cl_2$. Crystals of **3b** consist of $[Ph_2C_2N_3S]^+$ cations and $[PF_6]^-$ anions packed in a simple sodium chloride pattern.[20] Both the cation and anion lie on a crystallographic twofold axis. The C_2N_3S ring within the cation is planar to within 0.024 Å. The two phenyl rings are planar to within 0.003 Å, and the dihedral angle between the heterocyclic plane and the phenyl groups is 6.5°. Crystals of **5** consist of $Ph_2C_2N_3SH$ molecules weakly connected through hydrogen bonds between N1 (d(N1–H) = 2.29 Å) and N2 (d(N2–H) = 0.8 Å) of an adjacent molecule. In contrast to the cation, the C_2N_3S ring is now markedly nonplanar, adopting a boatlike or folded-book conformation. The protonated nitrogen N2 and the sulfur atom lie 0.296 (5) and 0.504 (2) Å out of the plane of the remaining ring atoms. The dihedral angle (the folded-book angle) between the planes N2–C1–N1–S and N2–C8–N3–S (both planar to within 0.023 Å) of 146° can be compared to the corresponding angle in the recently reported 3,5-diphenyl-1,4,2,6-dithiadiazine **6** (128.6°)[21] and the corresponding 1,4,2,5-dithiadiazine **7** (148.9°).[22]

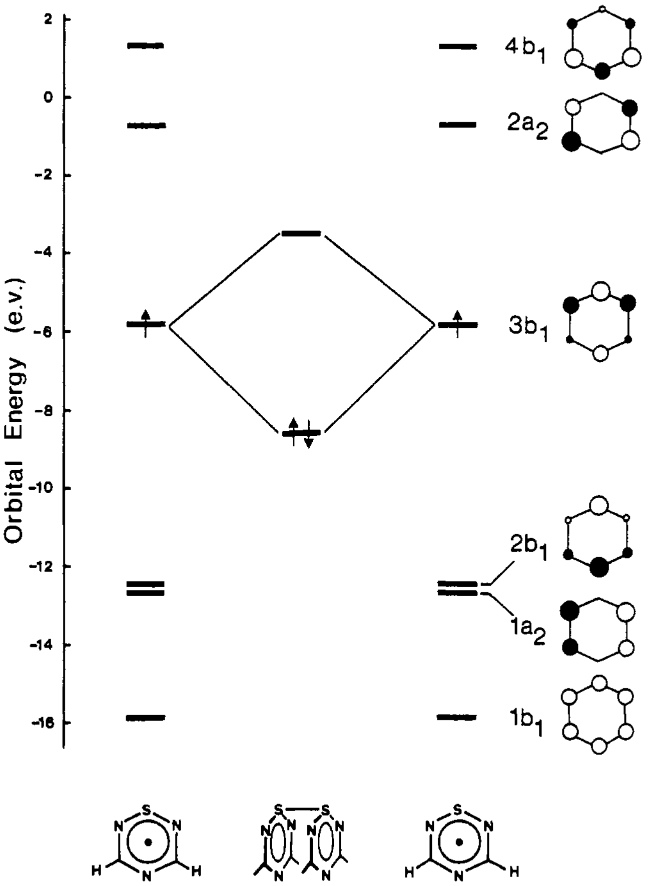

Figure 3. MNDO π molecular orbitals of $H_2C_2N_3S^•$, illustrating the interaction of two $3b_1$ SOMO's to form the S–S bond in the dimer $(H_2C_2N_3S)_2$.

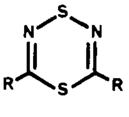

6

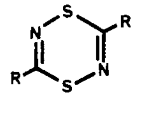

7

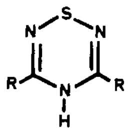

8

In addition to the conformational variations noted above there are major changes in the structural parameters within the C_2N_3S ring as a function of oxidation state. These trends are highlighted in Table V, which provides a comparison of the three chemically unique bond types in a variety of thiatriazine derivatives.[15,23] Although the long C–N2 and S–N1 bonds in **5** are easily interpretable, in a valence bond context, in terms of the dominance of the resonance structure **8**, the structural changes are more easily discussed in the light of the π-electron molecular orbital distributions within the C_2N_3S ring.

MNDO Calculations on $[H_2C_2N_3S]^+$, $H_2C_2N_3S^•$, and $[H_2C_2N_3S]^-$. The stability of the triad of oxidation states for the C_2N_3S ring, i.e. cation **3**, radical **1**, and anion **4**, is reminiscent of the well-known properties of odd-alternant hydrocarbons. In these latter compounds the SOMO of the radical is a non degenerate non-bonding distribution. Addition of an electron to this orbital to produce the anion, or removal of an electron from it to form the

---

(20) We also examined the BF_4^- salt **3a**. Eight crystals were considered and data sets collected on three. Unsatisfactory refinement because of BF_4^- disorder was always encountered. The unit cell was triclinic, $P\bar{1}$, with $a = 7.526$ (4) Å, $b = 10.199$ (6) Å, $c = 10.781$ (6) Å, $\alpha = 65.08$ (5)°, $\beta = 74.89$ (5)°, $\gamma = 87.69$ (5)°, and $Z = 2$. The best refinement ($R = 14\%$) gave a cation with bond distances and angles within a few standard deviations of those of the cation reported here.

(21) Daley, S. T. A. K.; Rees, C. W.; Williams, D. J. *J. Chem. Soc., Chem. Commun.* **1984**, 57.

(22) Smits, J. M. M.; Beurskens, P. T.; Lenz, B. G.; Zwanenburg. *Acta Crystallogr., Sect. C: Cryst. Struct. Commun.* **1985**, *C41*, 1086.

(23) Kalman, A.; Argay, G.; Fischer, E.; Rembarz, G. *Acta Crystallogr., Sect. B: Struct. Crystallogr. Cryst. Chem.* **1979**, *B35*, 860.

Table VI. MNDO π Charge Densities and Bond Orders and Net Charges ($\sigma + \pi$) for $H_2C_2N_3S$ (Cation, Radical, and Anion) and $H_2C_2N_3SH$

π Bond Orders

	S–N	N(2,6)–C	C–N(4)
cation	0.643	0.641	0.649
radical	0.350	0.745	0.573
anion	0.0736	0.899	0.499
$H_2C_2N_3SH$	0.153	0.916	0.317

π Charge Densities

	S	N(2,6)	C	N(4)
cation	1.197	1.140	0.724	1.075
radical	1.610	1.271	0.788	1.271
anion	1.974	1.424	0.817	1.544
$H_2C_2N_3SH$	1.931	1.253	0.876	1.811

Net Charges ($\sigma + \pi$)

	S	N(2,6)	C	N(4)
cation	+0.928	−0.325	+0.239	−0.175
radical	+0.444	−0.364	+0.177	−0.330
anion	+0.0219	−0.450	+0.167	−0.553
$H_2C_2N_3SH$[a]	+0.242	−0.332	+0.117	−0.416

[a] Net charge on H + 0.207.

cation, is therefore associated with relatively small structural and energetic changes. These features have prompted consideration of these systems in the design of one-dimensional metals.[24]

In the case of the thiatriazinyl system **1**, dimerization does not produce a stacked arrangement of C_2N_3S rings, e.g. **9**, although this does not preclude the possibility of such packing in related derivatives. The major difference between the present system and an odd-alternant hydrocarbon is the degree of occupancy of the π-orbital stack, i.e. the electron richness of the ring. In our description of the electronic structure of the $H_2C_2N_3S^{\bullet}$ radical we noted that the $3b_1$ SOMO is an antibonding distribution with respect to the S–N and opposite C–N linkages. The interaction of two singly occupied $3b_1$ orbitals on adjacent C_2N_3S rings is sufficient to produce a diamagnetic ground state for the dimer (Figure 3). This simplified orbital description of the dimer as a pair of radicals weakly coupled through their $3b_1$ SOMO's, a picture reminiscent of the electronic structure of the dithionite anion,[25] provides a useful framework for comparing the structural differences between **2**, **3**, and **5**. First, one could anticipate that oxidation or reduction of the C_2N_3S system would destabilize the dimeric structure (by respectively vacating the bonding orbital and filling the antibonding orbital in Figure 3). Second, the gradual lenghtening of the S–N and C–N(4) bonds and shortening of the C–N(2,6) bonds along the series **3**, **2**, and **5** could be interpreted as a response to the progressive occupation of the $3b_1$ orbital.

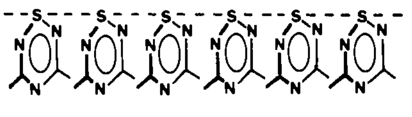

9

Table VII. MNDO Heats of Formation ΔH_f (kcal/mol) of the $H_2C_2N_3S$ Cation, Radical, and Anion Calculated by Using (a) the Optimized Geometry and (b) the Geometry of the Radical[a]

	a	b
cation	287.69	290.91
radical	76.27	76.27
anion	17.10	20.33

[a] Disproportionation energy (from (a)) 152 kcal/mol.

Quantitative MNDO molecular orbital calculations on model $[H_2C_2N_3S]^+$ and $[H_2C_2N_3S]^-$ ions reveal π-electron configurations and distributions that substantiate this simple one-electron picture. Table VI provides a bond order and charge distribution analysis for the triad of oxidation states of a $H_2C_2N_3S$ ring. Results relating to the protonated version of the anion, i.e. $H_2C_2N_3SH$, are also included. We begin the analysis of the results by confirming the continuity in the electron configurations of the different oxidation states; their π-electron counts differ only in the number of electrons in the $3b_1$ orbital. A calculation performed on the model anion with use of the triplet option of the MNDO program projected a heat of formation 28 kcal/mol higher than that of the singlet state. Second, we note that the bond order variations along the series cation, radical, and anion can be directly related to the extent of occupation of this orbital. Protonation of the anion to produce the imide further perturbs the system by polarizing the $3b_1$ orbital (inter alia) toward the site of protonation. We have observed similar effects during the protonation of the $S_3N_3^-$ anion to S_3N_3H.[26] In this latter case the polarization of antibonding electron density weakens the S–N(H) bonds to such an extent that collapse of the six-membered ring structure is induced (eq 1). The π system of the thiatriazine anion ring is less electron rich (i.e. contains fewer π electrons per atomic center) than is $S_3N_3^-$, so that sufficient structural stability is retained within the six-membered ring to resist bond rupture. Nonetheless, some puckering of the ring is to be expected, and the observed boatlike conformation of **5** confirms this idea. An MNDO calculation on a $H_2C_2N_3SH$ model in C_s symmetry produced a shape similar to that of **5** but reduced the ΔH_f value by less than 1 kcal/mol, indicating that the potential energy surface for the folding process is extremely shallow.

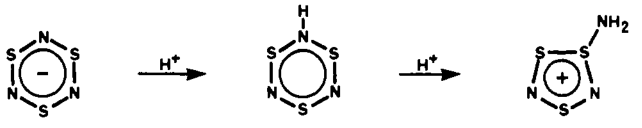

(1)

The π-electron densities ρ_π and net charges $q_{\sigma+\pi}$ calculated for our model compounds provide information as to how the C_2N_3S ring system responds to redox changes. Oxidation and reduction of the $H_2C_2N_3S$ radical both result in a significant reorganization; in the cation almost all the positive charge is accommodated by the π system at the sulfur atom; i.e., sulfur is more easily oxidized than nitrogen. Conversely in the anion the negative charge is concentrated on the three nitrogen atoms. Similar effects have been observed in binary sulfur–nitrogen rings; the oxidation of S_4N_4 to $S_4N_4^{2+}$ effects a charge removal from sulfur, while its reduction to $S_3N_3^-$ causes a charge buildup at nitrogen.[27] These changes reflect the greater atomic electronegativity of nitrogen compared to that of sulfur.

Thiatriazines as One-Dimensional Conductors. The potential utility of odd-alternant hydrocarbons in the design of one-dimensional conductors stems, in large part, from their low disproportionation energy (which can be correlated with the ionic fluctuation energy U_{eff}). This arises from the lower Coulombic resistance for charge transfer between two neutral radicals as opposed to that for two charged radicals, e.g. between two $TCNQ^-$ radical anions. In order to investigate the applications of thiatriazinyl radicals in this area, we have calculated the heats of formation of the different oxidation states of the C_2N_3S ring (Table VII), and from these data we estimate a disproportionation energy of 153 kcal/mol. This rather large value, which is some 50% greater than has been calculated for the phenalenyl radical[24] or TTF^+ or $TCNQ^-$,[28] stems principally from the expectedly high ionization potential of the radical. If inorganic heterocycles such

---

(24) (a) Haddon, R. C. *Aust. J. Chem.* **1975**, *28*, 2343. (b) Haddon, R. C. *Nature (London)* **1975**, *256*, 394.

(25) Dunitz, J. *Acta Crystallogr.* **1956**, *9*, 579.

(26) Marcellus, C. G.; Oakley, R. T.; Cordes, A. W.; Pennington, W. T. *Can. J. Chem.* **1984**, *62*, 1822.

(27) Trsic, M. T.; Laidlaw, W. T.; Oakley, R. T. *Can. J. Chem.* **1982**, *60*, 2281.

(28) Haddon, R. C. *Aust. J. Chem.* **1975**, *28*, 2333.

as those described here are to find applications in the design of low-dimensional conductors, this detrimental feature must be overcome.

Summary

In contrast to the behavior of binary sulfur–nitrogen ring systems, the six-membered 1,2,4,6-thiatriazine unit is stable to both oxidation and reduction. Examples of the three oxidation states—cation, neutral radical, and anion (in its protonated form)—have been structurally characterized. The structural and energetic differences between the different oxidation states can be understood in terms of the degree of occupation of the π manifold of the C_2N_3S ring.

Acknowledgment. We thank the Natural Sciences and Engineering Research Council of Canada, Research Corp., the National Science Foundation (EPSCOR Grant ISP 801147), and the State of Arkansas for financial support of this work. R.T.B. acknowledges the NSERCC for a postdoctoral fellowship.

Registry No. **2**, 94405-47-7; **3a**, 102420-46-2; **3b**, 102420-47-3; **5**, 102420-48-4; $Ph_2C_2N_3SH{\cdot}CH_2Cl_2$, 102420-49-5; $Ph_2C_2N_3SCl$, 94426-38-7; $Ph_2C_2N_3SNMe_2$, 102420-50-8; Me_2NSiMe_3, 2083-91-2; $H_2C_2N_3S^+$, 102420-51-9; $H_2C_2N_3S^\bullet$, 102535-02-4; $H_2C_2N_3S^-$, 102420-52-0; $H_2C_2N_3SH$, 290-94-8.

Supplementary Material Available: Anisotropic thermal parameters (Tables S1 and S2) for structures **3b** and **5** (2 pages). Ordering information is available on any current masthead page.

Contribution from the Department of Chemistry,
University of Houston, University Park, Houston, Texas 77004

Oxidative Alkylation of Cobalt Complexes with Hydrazines

E. G. Samsel and J. K. Kochi*

Received December 18, 1985

Cobalt complexes related to the salen ligand [*N,N'*-ethylenebis(salicylideneaminato)] are efficiently converted to the corresponding organocobalt(III) derivative such as RCo^{III}(salen) by various hydrazines ($RNHNH_2$) under oxidative conditions with either dioxygen or *tert*-butyl hydroperoxide. Optimum conditions are developed for the oxidative alkylation of various cobalt complexes with structurally diverse hydrazines. The limitations of the hydrazine method are delineated and accounted for by a study of the stoichiometry and reactive intermediates. Foremost among the latter are the superoxo and *tert*-butylperoxo complexes of cobalt(III) derived by oxidation, ligand exchange, or ligand-induced homolysis of different cobalt(II) and cobalt(III) precursors. Such cobalt(III) oxidants are responsible for the two-electron conversion of alkylhydrazines to their diazene derivatives. The subsequent extrusion of dinitrogen affords the organic radical ($R\cdot$) as the key intermediate responsible for the alkylation of the cobalt(II) center. The primacy of alkyl radicals in the hydrazine procedure is established with the chemical clock utilizing the unimolecular homolytic rearrangement of 5-hexenyl to cyclopentylmethyl.

Introduction

A variety of synthetic methodologies is now available for the preparation of different metal–alkyl complexes.[1,2] However, those procedures that utilize oxidizing conditions are rare—a notable exception being the alkylation of chromium(II) complexes with organic hydroperoxides.[3] Thus the reports that various macrocyclic complexes of cobalt, iron, chromium, and manganese can be converted by organic hydrazines to the corresponding alkyl and aryl derivatives with air as a reagent are especially intriguing.[4-8] Accordingly, we have examined the oxidative synthesis of a variety of organocobalt complexes with different types of hydrazines. Our primary focus in this study is to delineate the reaction conditions, the stoichiometry, and the intermediates in the oxidative alkylation.

Table I. Oxidative Methylation of Co^{II}(salen) with Methylhydrazine[a]

$[CH_3NHNH_2]$, mM	oxidant (concn, mM)	temp, °C	[MeCo(salen)], mM (%)[b]
21	O_2[c]	22	14.0 (57)
42	O_2[c]	22	15.3 (73)
105	O_2[c]	22	17.8 (85)
210	O_2[c]	22	16.6 (79)
105	O_2[c]	0	17.7 (84)
105	O_2[c]	45	18.6 (89)
105	O_2[c,d]	22	17.8 (85)
105	*t*-BuOOH (52)[e]	22	18.4 (88)
105	PhIO (52)[e]	22	11.6 (55)
105	$3\text{-}ClC_6H_4CO_3H$ (46)[e]	22	0 (0)

[a] In 5 mL CH_2Cl_2 containing 2.1×10^{-2} M Co(salen) (I). [b] Based on I charged; isolated as the pyridine complex. [c] 1 atm of pure dioxygen. [d] Reverse addition of CH_3NHNH_2 to I and O_2. [e] Oxidant added to I and CH_3NHNH_2 under an argon atmosphere.

We selected the cobalt complexes that are derived mainly from salen [I, *N,N'*-ethylenebis(salicylideneaminato)] in view of the extensive preparative chemistry extant for (alkyl)- and (aryl)-Co^{III}(salen) complexes.[9] In order to provide some scope, the alkylations of the related Schiff base complexes of cobalt(II) with the ligands saloph (II), dmgH (III), and acacen (IV) are also reported. The formation of organic radicals as the reactive in-

---

(1) Cotton, F. A.; Wilkinson, G. *Advanced Inorganic Chemistry*, 4th ed.; Wiley: New York, 1980; pp 1133–8.
(2) Collman, J. P.; Hegedus, L. S. *Principles and Applications of Organotransition Metal Chemistry*; University Science: Mill Valley, CA, 1980; Chapter 11.
(3) Espenson, J. H. *Adv. Inorg. Bioinorg. Mech.* **1982**; *1*, 1–63.
(4) Braunstein, P. *J. Chem. Soc., Chem. Commun.* **1973**, 851. Braunstein, P.; Clark, R. J. H. *J. Chem. Soc., Dalton Trans.* **1973**, 1845; *Inorg. Chem.* **1974**, *13*, 2224.
(5) Goedken, V. L.; Peng, S.-M.; Park, Y. *J. Am. Chem. Soc.* **1974**, *96*, 284. Goedken, V. L.; Peng, S.-M. *Ibid.* **1974**, *96*, 7826. Goedken, V. L.; Peng, S.-M. *J. Chem. Soc., Chem. Commun.* **1975**, 258.
(6) Dey, K.; De, R. L. *J. Inorg. Nucl. Chem.* **1977**, *39*, 153.
(7) Battioni, P.; Mahy, J. P.; Gillet, G.; Mansuy, D. *J. Am. Chem. Soc.* **1983**, *105*, 1399.
(8) (a) Mansuy, D.; Battioni, P.; Mahy, J.-P.; Gillet, G. *Biochem. Biophys. Res. Commun.* **1982**, *106*, 30. (b) Kunze, K. L.; Ortiz de Montellano, P. O. *J. Am. Chem. Soc.* **1983**, *105*, 1380. (c) See also: Hill, H. A. O.; Thornalley, P. J. *FEBS Lett.* **1981**, *125*, 235.
(9) For reviews see: (a) Kemmitt, R. D. W.; Russell, D. R. In *Comprehensive Organometallic Chemistry*; Wilkinson, G., Stone, G. F. A., Abel, E. W., Eds.; Pergamon: New York, 1982; Vol. 5, p 1. (b) Dodd, D.; Johnson, M. D. *J. Organomet. Chem.* **1973**, *52*, 1. (c) Pratt, J. M.; Craig, P. J. *Adv. Organomet. Chem.* **1973**, *11*, 331.